Second-order advantage achieved by modeling excitation–emission fluorescence matrices affected by inner filter effects using a strategy which combines standardization and calibration: Reducing experimental and increasing analytical sensitivity

Agustina V. Schenone [a], María J. Culzoni [a], María Martínez Galera [b], Héctor C. Goicoechea [a,*]

[a] *Laboratorio de Desarrollo Analítico y Quimiometría (LADAQ), Cátedra de Química Analítica I, Facultad de Bioquímica y Ciencias Biológicas, Universidad Nacional del Litoral—CONICET, Ciudad Universitaria, Santa Fe S3000ZAA, Argentina*
[b] *Departamento de Química y Física, Campus de Excelencia Agroalimentario CeiA3, Facultad de Ciencias Experimentales, Universidad de Almería, La Cañada de San Urbano, 04120 Almería, Spain*

ARTICLE INFO

ABSTRACT

A methodology based on second-order data (excitation emission matrices) modeling with one of most popular algorithms presenting the second-order advantage, parallel factor analysis (PARAFAC), combined with transference of calibration is proposed to predict the analyte concentration when significant inner filter effects occur, even in the presence of unexpected sample components.

The quantitation of phenylephrine hydrochloride (PHE) in water samples (concentrations ranged between 250 and 750 ng mL^{-1}) in the presence of ibuprofen, acetyl salicylic acid and paracetamol (which produce inner filter effect across the useful wavelength range) was achieved. The strategy allows reducing the experimental work and increasing the analytical sensitivity in the determination of the analyte of interest in the presence of unexpected compounds and matrix effect caused by inner filter, avoiding the preparation of a large number of solutions and maintaining acceptable figures of merit. Recoveries between 97 and 102% for validation and real spiked water samples, respectively, and a relative prediction error of 5% were achieved.

Results were compared with those obtained after the application of the classical standard addition method combined with PARAFAC, carrying out five additions to each sample, in triplicate. The presented methodology constitutes a simple and low-cost method for the determination of PHE in water samples with a considerable reduction in standard handling and time. This methodology can be extended to other systems presenting matrix effect and, consequently, can become in a useful tool to know the amount of pharmaceuticals in the aquatic environment and to evaluate the effect of conventional wastewater treatment plants in the elimination of pharmaceutical compounds.

© 2013 Elsevier B.V. All rights reserved.

1. Introduction

Generally, the determination of pharmaceutical compounds in complex samples requires the application of different methodologies in order to obtain selectivity when unexpected compounds are present and, also, to deal with matrix effect, which involves changes (enhancement or suppression) in the analytical response (with respect to that found in clean or less complex samples). In these cases, a calibration curve based on pure analyte samples will furnish an incorrect determination [1].

An inherent problem of many fluorimetric procedures is the absorption of exciting and/or emitted radiation by dissolved species (either fluorescent or not) or by the fluorophore itself [2]. This is termed the inner filter effect and leads to a variation not only in intensity but also in spectrum shape. Both drawbacks can be corrected by the well known standard addition method (SAM), which compensates matrix effects arising from the specific composition of the sample. However, the major inconvenient linked to this methodology is the high number of experiments needed, as new calibration curves must be built when new samples are analyzed. Furthermore, in order to accomplish acceptable figures of merit, it is highly recommended that at least four different concentrations of pure standard should be added to the sample [1–3]. On the other hand, given a multicomponent mixture with several analytes of interest, generalized standard addition method (GSAM) is required

to simultaneously determine the analyte concentrations [4], mostly according to an experimental design [5]. Several interesting applications have been developed in this context [5–8].

As mentioned above, real sample composition often includes undesirable compounds. These multicomponent mixtures can be solved with multivariate calibration techniques such as partial least squares (PLS-1). However, with the aim of achieving precision and accuracy, first order algorithms need to model not only all the responsive components, but the whole matrix effect in the calibration step by preparing a large number of samples [9].

It is known that analyte quantitation in the presence of responsive potential interferents can be performed by measuring second-order signals and processing them with appropriate second-order multivariate algorithms achieving the second-order advantage [10]. Combinations of these algorithms and SAM have been proposed to solve both inconveniences: presence of unknown components and matrix effect. Several applications of PARAFAC have been published in the literature [11–14], when the sensitivity of the response depends on the matrix composition. Other second-order calibration algorithms being used in this context were multivariate curve resolution based on alternating least squares (MCR-ALS) [15–17], as well as self-weighted alternating trilinear decomposition (SWATLD) [18] and multidimensional partial least squares model coupled to residual bilinearization (N-PLS/RBL) [19]. Nevertheless, in all cases, a high number of samples still need to be prepared to reach acceptable figures of merit.

Recently, the ability of U-PLS/RBL to analyze complex samples of fluorescent species showing inner filter effects was demonstrated [20,21]. Interestingly, the time-consuming experimental procedure for SAM was avoided modeling the spectral changes through the flexibility of PLS. However, in these cases, both the analyte and the component causing inner filter effect were modeled in the calibration step, therefore being necessary to know the component that causes this effect, which cannot be easily achieved in most real samples.

The main purpose of the strategy presented in this work is to reduce the number of samples to be prepared when interferences and inner filter effect are present together in a sample without the requirement of knowing the sample composition.

In order to solve the first task, the well-known algorithm PARAFAC was applied to obtain the analyte signal free from those generated by components not included in the calibration set. To overcome the inner filter effect with minimum sample preparation, a novel approach has been implemented, i.e., second-order modeling coupled to calibration transfer. Standardization techniques are mostly used to transfer a calibration model created in one instrument to a new situation (i.e., a different instrument, altered conditions, etc.), thereby avoiding full recalibration [22]. Various methods for calibration transfer exist in the literature attempting to deal with noncalibrated variations that are detected after the model is already in use (i.e., change of the instrument or a part of it) [23–25]. An important development in multivariate transfer is piecewise direct standardization (PDS) [26], which reconstructs each spectral point on the primary instrument from several measurements in a small window on the secondary instrument. Some reports have been published regarding the application of PDS in several contexts, such as classification [27], correction of spectral variation induced by temperature [28] and calibration transfer for three-way data structures [29]. A literature search reveals that PDS can be considered the routine method for calibration transfer.

We and other authors have previously reported the combination of PDS with second order modeling to alleviate the experimental work [30–32]. These latter publications corresponded to high performance liquid chromatography with diode array detection (HPLC-DADS) applications for determination of emergent contaminants in water samples. Transferred calibration data sets were obtained from standardization of solvent based calibration data and used in the prediction step of water samples in which the matrix effect was evident owing to the SPE step which needs considerable both time and chemicals. As a result, the chromatographic profiles obtained by direct injection could be standardized into chromatograms in real situations using transfer vector with high determination coefficients among signals before and after transformation ($r^2 \geq 0.99$). In the present report effort was put in performing a full statistical demonstration of the applicability and robustness of the proposed methodology. Whit this aim, a set of simulated and experimental excitation–emission matrices (EEM) data were created in order to evaluate the performance of the methods. In addition, an experimental system was used to determine phenylephrine hydrochloride (PHE) in water samples in the presence of ibuprofen (IBU), acetyl salicylic acid (ASA) and paracetamol (PAR). PHE has been previously determined in several pharmaceutical forms by HPLC [33,34], flow injection analysis [35], spectrophotometry [36], capillary electrophoresis [37], spectrofluorometry [38] and multivariate calibration by using PLS-1 modeling [39]. It has been demonstrated that in the presence of PAR, the emission intensity of PHE strongly decreases, due to the high absorbance of PAR across the excitation maximum of PHE [5,38]. For these reasons, a novel chemometric strategy was developed. The methodology first applies PDS to unfolded matrices in order to transfer the sample signal to the calibration curve conditions using only two standard samples in each situation. Afterwards, the refolded transferred data is subjected to PARAFAC modeling in order to obtain the scores useful for analyte prediction (PDS/PARAFAC). An additional advantage (in addition to the fact that only two standard additions are needed) is achieved when these methods are applied, since the analytical sensitivity of the calibration curve is kept and the sample signal is transferred in order to be predicted using the standard curve. Results were compared with those obtained after the application of standard addition method combined with PARAFAC, carrying out five additions to the sample in triplicate.

2. Experimental

2.1. Reagents and solutions

PHE, IBU, ASA and PAR were obtained from Laboratory of Pharmaceutical Quality Control (Faculty of Biochemistry and Biological Sciences, National University of Litoral, Argentina). Aqueous stock solutions of PHE (100 mg L^{-1}), ASA (100 mg L^{-1}) and PAR (200 mg L^{-1}) were prepared. IBU 100 mg L^{-1} was prepared in methanol of HPLC grade (Aberkon, Buenos Aires, Argentina). An aliquot of 1.00 mL of the latter solution was placed into a 10.00 mL volumetric flask, the solvent was evaporated to dryness by a gentle stream of nitrogen and the flask was then completed to the mark with Milli-Q water. Ultrapure water was obtained from a Milli-Q water purification system from Millipore (Bedford, MA, USA).

2.2. Apparatus

All spectrofluorimetric measurements were performed using a Perkin-Elmer LS-55 luminescence spectrometer equipped with a Xenon discharge lamp, Monk-Gillieson type monochromators and a gated photomultiplier connected to a PC microcomputer via a RS232C connection and using 1.00 cm quartz cells. Excitation–emission fluorescence matrices were collected varying the excitation wavelength between 215 and 240 nm each 2 nm, and

registering the emission spectra from 270 to 360 nm each 0.5 nm. Hence, the size of each data matrix was 181×13. The slit band widths for the excitation and emission monochromators were fixed at 10 nm and the detector voltage at 650 V.

For data processing, all implemented routines were performed using the software MATLAB 7.1 [40] and the PLS_Toolbox 2.1.1. from Eigenvector Inc. [41]. A useful interface for data input and parameters setting, written by Olivieri et al. [42] was employed for PARAFAC implementation.

2.3. Data

2.3.1. Simulated data

Simulated excitation–emission data were used to study the performance of the present strategy. A calibration set of second-order signals was built with a single analyte at nominal concentrations from 1.0 to 6.0 (in arbitrary units) each 1 unit, in triplicate. A test set was also created with 51 test samples in which one uncalibrated component was included together with the calibrated analyte, the latter at nominal concentrations from 1.0 to 6.0 each 0.1. The uncalibrated compound simulates not only an interferent but also causes inner filter effect, decreasing the fluorescence intensity of the original signal at any channel, and modifying the emission analyte profiles, which vary across the set of samples. Moreover, six analyte additions from 1.0 to 6.0 were done for each of the test samples in triplicate.

The dimension of each data matrix was 31×31 data points (corresponding to the first and second dimension, which is intended to mimic emission and excitation wavelengths, respectively). The level of noise added to the simulated second-order data was 1% and 5% in signal and concentration, respectively. Fig. 1 shows the excitation and emission spectra of components 1 and 2 and ilustrates how the analyte profiles in both dimensions vary in a test sample.

In the absence of inner filter effects, the calibration signals would be computed as:

$$\mathbf{X}_{c,i} = y_{1,c,i}\,\mathbf{S}_1 + \mathbf{R}\,s_X \tag{1}$$

in which $\mathbf{X}_{c,i}$ is the $J \times K$ matrix of second-order signals for the ith calibration sample, $y_{n,c,i}$ is the nominal concentration of each analyte, and $\mathbf{S}_n = k_n\,\mathbf{b}_n\,\mathbf{c}_n^T$ are the corresponding matrix signals at unit concentration for the analyte n ($\mathbf{b}_n$ and $\mathbf{c}_n$ are the profiles in the first and second dimensions, both normalized to unit length, and k_n is a scaling factor, all set at 1), $\mathbf{R}$ is a matrix of Gaussian random numbers with unit standard deviation of appropriate size, and s_X is the standard deviation of the noise added to signals.

The test signals were built using the following expression:

$$\mathbf{X}_u = y_{1,u}\,\mathbf{S}_1 + y_{2,u}\,\mathbf{S}_2 + \mathbf{R}\,s_X \tag{2}$$

where $\mathbf{X}_u$ is the $J \times K$ matrix for the unknown sample, $y_{n,u}$ is the nominal concentration of each component, and $\mathbf{S}_2$ is the matrix signal for the unexpected component.

When inner filter effect from component 2 on component 1 is present, then $\mathbf{S}_1$ is replaced in Eq. (2) by an $\mathbf{S}_{1,\mathrm{if}}$ matrix whose generic (j,k) element is given by the following expression:

$$\mathbf{S}_{1,\mathrm{if}}(j,k) = \mathbf{S}_1(j,k) \times \exp[-(\varepsilon_{2j} + \varepsilon_{2k})y_{2,u}] \tag{3}$$

in which ε_{2j} and ε_{2k} are the absorptivities of component 2 at channels j and k, respectively, in each of the data dimensions. The product $(\varepsilon_{2j}\,y_{2,u})$ represents the inner filter effect produced when component 2 absorbs the excitation intensity at channel j, whereas $(\varepsilon_{2k}y_{2,u})$ corresponds to absorption of the emission intensity at channel k. The absorptivities are given by the product of an adjustable scaling factor and the values of the excitation profile $\mathbf{c}_2$ at each of these two channels.

2.3.2. Experimental data

2.3.2.1. Sample collection and preparation.
Well water and tap water were collected from Santa Fe (Argentina). Before analysis they were centrifuged at $5000 \times g$, filtered through 0.45 μm filters and stored at 4 °C in refrigerator.

2.3.2.2. Preparation of standards and spiked samples.
A calibration curve of five standard samples of PHE was prepared in the range from 250 to 750 ng mL^{-1} each 125 ng mL^{-1}, in triplicate. Furthermore, the
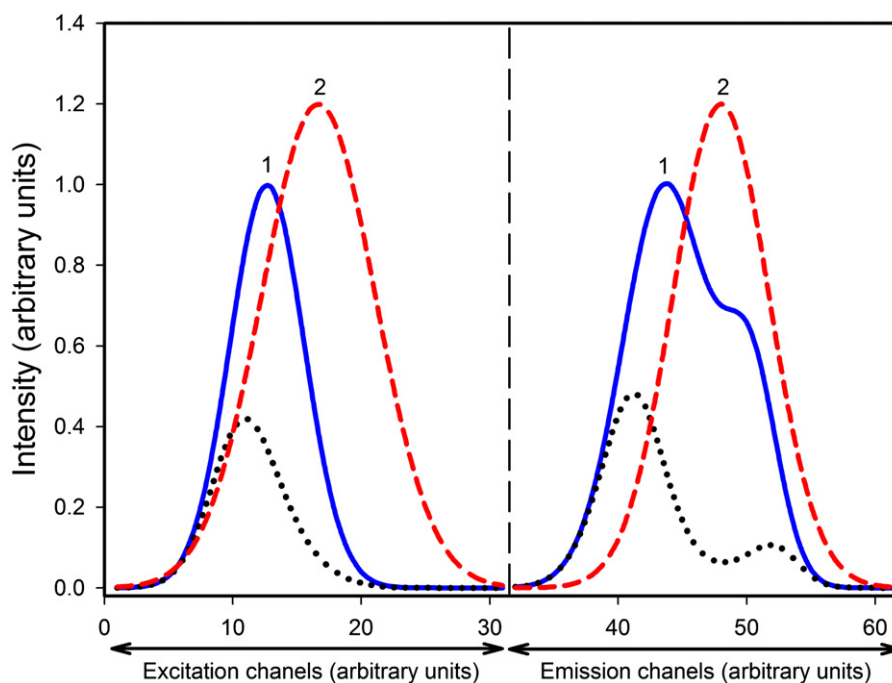

Fig. 1. Simulated excitation and emission profiles for pure component 1 (solid line) and 2 (dashed line) and component 1 in a test sample after computing the inner filter effect produced by component 2 in both dimensions (dotted line).

same set of samples was prepared in the presence of 10.00 mg L^{-1} of PAR in order to compare the slope of both regressions.

Following a fractional central composite design of four factors at five levels, a validation set of seventeen samples was prepared in Milli-Q water with different concentrations of PHE (from 248 to 400 ng mL^{-1}), IBU (from 251 to 400 ng mL^{-1}), ASA (from 50 to 79 ng mL^{-1}) and PAR (from 5.0 to 20.0 mg L^{-1}). Composition of the validation samples is shown in Table 1.

Well water and tap water samples, treated as described above, were spiked with PHE, IBU, ASA and PAR at different concentration levels. The composition of these samples is explained below in the 'Results and discussion' section.

Two additions of PHE stock solution were made to each validation and water sample (375 and 625 ng mL^{-1}) in order to implement the transference procedure. Moreover, five additions (from 250 to 750 ng mL^{-1}) of analyte stock solution were carried out in triplicate to three of the test samples (samples 2, 12 and 14 from Table 1) to apply the standard addition method.

Samples were prepared by measuring appropriate aliquots of standard solutions of each drug, placing them into 10.00 mL volumetric flasks to obtain the desired concentrations and completing to the mark with Milli-Q water or with each sample in the case of validation samples and water samples, respectively.

3. Theory

3.1. PDS

In the present report, a combination of second-order algorithm and piecewise direct standardization (PDS) [26] was used in order to isolate the analyte signal and to transform the sample data into the signal corresponding to pure analyte situation, respectively. As a consequence, an additional advantage is achieved since the analytical sensitivity of the response will be that corresponding to the calibration curve made with pure standards instead of the one from the curve with inner filter effect.

PDS relates the response **r** of a sample obtained in a situation A (**X**$_A$) to the response obtained in a situation B (**X**$_B$), the relationship being described by the transformation matrix **F**, according

Table 1
Composition of the experimetal validation set*.

Sample	PHE (ng mL^{-1})[a]	IBU (ng mL^{-1})[a]	AAS (ng mL^{-1})[b]	PAR (mg L^{-1})[c]
1	365.0	369.6	54.5	8.04
2	365.0	280.0	74.3	12.5
3	321.2	400.4	64.4	20.0
4	277.4	369.6	54.5	12.5
5	321.2	324.8	79.2	17.0
6	394.2	324.8	64.4	8.04
7	277.4	280.0	54.5	12.5
8	365.0	369.6	74.3	8.04
9	321.2	324.8	64.4	17.0
10	321.2	324.8	64.4	12.5
11	365.0	280.0	54.5	12.5
12	248.2	324.8	64.4	17.0
13	321.2	250.6	64.4	12.5
14	321.2	324.8	49.5	5.0
15	321.2	324.8	64.4	12.5
16	277.4	369.6	74.3	8.04
17	277.4	280.0	74.3	17.0

* Following a fractional central composite design of four factors at five levels.
[a] Uncertainty in concentration s=7 ng mL^{-1} estimated by error propagation.
[b] Uncertainty in concentration s=6 ng mL^{-1} estimated by error propagation.
[c] Uncertainty in concentration s=0.1 mg L^{-1} estimated by error propagation.

to:

$$\mathbf{X}_A = \mathbf{X}_B \mathbf{F} \tag{4}$$

In the case under study, situation A corresponds to excitation–emission signals from standards built in Milli-Q water and situation B to excitation–emission signals with inner filter effect.

PDS builds a multivariate model between the response **r** of a sample measured at the jth wavelength in situation A and different responses obtained in situation B. These secondary responses are in a window that is centered in the jth wavelength. The relationship can be described as follows:

$$\mathbf{r}_j = \mathbf{R}_j \mathbf{b}_j \tag{5}$$

in which **R**$_j$ is the localized response matrix of the transfer samples and **b**$_j$ is the vector of transformation coefficients for the jth tensor. The regression vectors calculated for each window in the data are then assembled to form a banded diagonal matrix **F**, according to

$$\mathbf{F} = \mathrm{diag}(\mathbf{b}_1^T, \ \mathbf{b}_2^T, \ldots, \ \mathbf{b}_j^T, \ldots, \ \mathbf{b}_k^T) \tag{6}$$

in which k is the number of sensors. In the case under study, **F** matrix was calculated using only two samples in each situation and window size equal to three. The samples in situation A were two pure standard samples (2 and 5 in arbitrary units for simulated data, 375 and 625 ng mL^{-1} for experimetal data) and in situation B, two additions made to the sample (in the same levels as the standards) in the presence of inner filter effect. The response of any unknown sample can then be standardized according to:

$$\mathbf{x}_S^T = \mathbf{x}^T \mathbf{F} \tag{7}$$

in which **x**$_S^T$ represents the sample as if it would have been measured under situation A (absence of inner filter effect).

As can be seen, the explained methodology is suitable for first order signals. Consequently, data matrices were first unfolded into two-way data and subjected to PDS, followed by the application of PARAFAC to the refolded transfered matrices. The gathered scores were then useful for sample prediction (see Fig. 2).

3.2. PARAFAC

The strategy presented in this report combines PDS with PARAFAC. This was carried out by first unfolding the EEM into vectors and then submiting them to PDS as explained in Section 3.1. Once the sample data was transferred to the calibration curve situation, the refolded matrices were subjected to PARAFAC (see Fig. 2).

A PARAFAC model of a three-way array is given by three loading matrices, **A**, **B**, and **C** with elements a_{in}, b_{jn}, and c_{kn} [43]. The trilinear model is found to minimize the sum of squares of the residuals, e_{ijk} in the model:

$$x_{ijk} = \sum_{n=1}^{N} a_{in} b_{jn} c_{kn} + e_{ijk} \quad i=1,2,\ldots, I, \quad j=1,2,\ldots, J, \quad k=1,2,\ldots,K \tag{8}$$

The matrix form of this trilinear model is as follows:

$$\mathbf{X}_k = \mathbf{A} \ \mathrm{diag}(\mathbf{c}_{(k)}) \mathbf{B}^T + \mathbf{E}_k \quad k=1,2,\ldots, K \tag{9}$$

In chemistry, the columns of the loading matrices **A** and **B** can always be assigned with certain physical meanings, i.e., excitation and emission spectra in fluorescence spectrometry, and chromatographic profiles and ultraviolet–visible spectra in HPLC-DAD. The columns of the loading matrix **C** often represent concentrations of components in mixtures.

In second-order calibration, PARAFAC first treats all the loading matrices **A**, **B** and **C** as unknowns. Then, they are estimated by
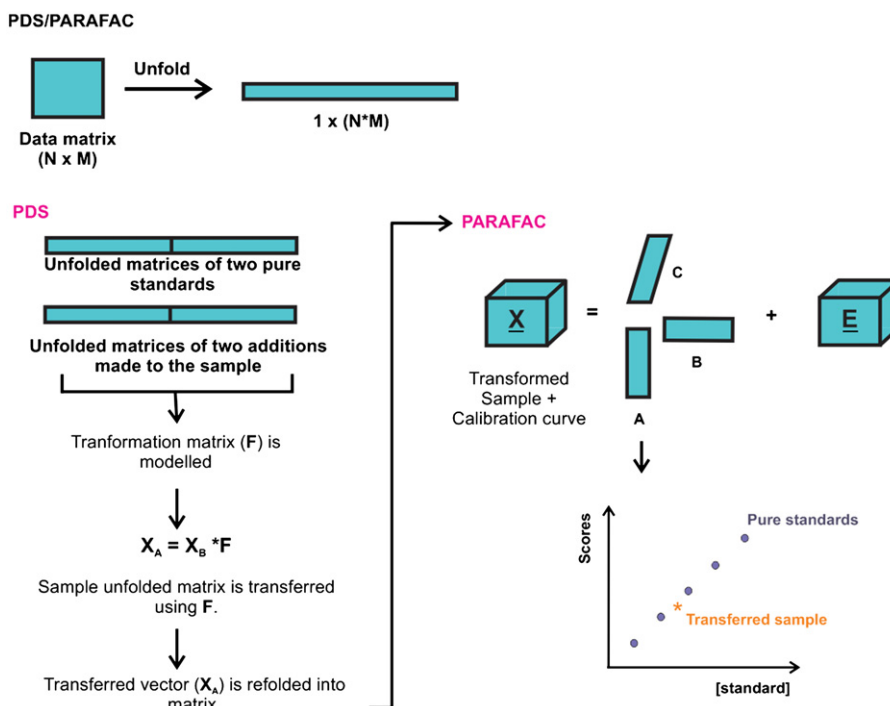
Fig. 2. Diagram indicating how predictions are made by PDS/PARAFAC on a new test sample containing unexpected components and inner filter effect. See text for details on the employed symbols.

alternating least squares algorithm after random initialization. The concentrations of the components in unknown samples are predicted by regressing the loading matrix **C** estimated by PARAFAC on the known concentrations of the calibration samples.

When the standard addition method is combined with PARAFAC, the raw second-order data of the sample and that of each five additions in triplicate are analyzed together. The estimation of the analyte concentration in the sample can be obtained through a plot of the scores (sample mode loadings in **C**) as a function of the amount of standard added by fitting a line to the data and finding its intercept on the abscissa, in the same way as in univariate standard addition.

4. Results and discussion

4.1. Simulated data

For illustrating the performance of the developed method, simulated excitation–emission data with two components, a given noise level and inner filter effect were built (see 'Experimental' section).

The second-order data for each of the 51 test samples was treated as follow: first, the data from a test sample and two additions (2 and 5) as well as two samples from the calibration curve were unfolded into vectors. After that, the sample vector was subtracted from the vectors of each of the two additions made to this sample. PDS was then applied to obtain **F** using a window size equal to three and a tolerance equal to 0.01. This transformation matrix was then used to transfer the sample unfolded data matrix. The new sample signal was refolded into a matrix and subjected to PARAFAC together with the standard curve and the scores were used for sample prediction. The number of PARAFAC factors for these samples was determined through the analysis of the core consistency [44], which allows establishing it as two in samples with the interference.

The transformation impact can be appreciated in Fig. 3, which shows the contour plots of the same simulated test sample before and after PDS/PARAFAC and are compared with the pure analyte signal. The standard addition method, combined with PARAFAC, was also applied to simulated data in order to compare the results gathered with the method described in this work.

Prediction parameters from the 51 simulated samples are summarized in Table 2. Prediction results were satisfactory, leading to mean recovery of 100.0% and a relative error of prediction (REP) of 3.7% for PDS/PARAFAC. Interestingly, when applying the classical SAM combined with the second-order algorithm, the results obtained were of the same quality, showing that the experimental work can be considerably reduced.

The estimation of figures of merit in multi-way calibration has been subject of several papers in the recent literature [45–47]. Sensitivity (SEN), defined as the change in net response for a given change in analyte concentration, can be considered as one of the most relevant in the scenario of analytical chemistry owing it is a decisive factor in estimating other figures of merit, such as limit of detection (LOD), limit of quantitation (LOQ) and uncertainty in prediction of concentration (SD) [45].

According to Olivieri and Faber [47], a general expression for computing the sensitivity in any calibration situation using second-order bilinear signals can be obtained as:

$$\text{SEN}n = sn \left\{ \left[(\mathbf{B}_{exp}{}^{T} \mathbf{P}_{b,\ unx} \mathbf{B}_{exp}) * (\mathbf{C}_{exp}{}^{T} \mathbf{P}_{c,\ unx} \mathbf{C}_{exp}) \right]^{-1} \right\}_{nn}^{-1/2} \quad (10)$$

in which '$*$' indicates the element-wise Hadamard matrix product, 'nn' implies the (n,n) element of a given matrix and sn is the integrated total signal for component n at unit concentration. $\mathbf{B}_{exp}$ and $\mathbf{C}_{exp}$ are the expected sample components that are present in the calibration set of samples, and $\mathbf{P}_{b,unx}$ and $\mathbf{P}_{c,unx}$ can be obtained by the following expressions:

$$\mathbf{P}_{b,\ unx} = \mathbf{I} - \mathbf{B}_{unx} \quad (11)$$

$$\mathbf{P}_{c,\ unx} = \mathbf{I} - \mathbf{C}_{unx} \quad (12)$$
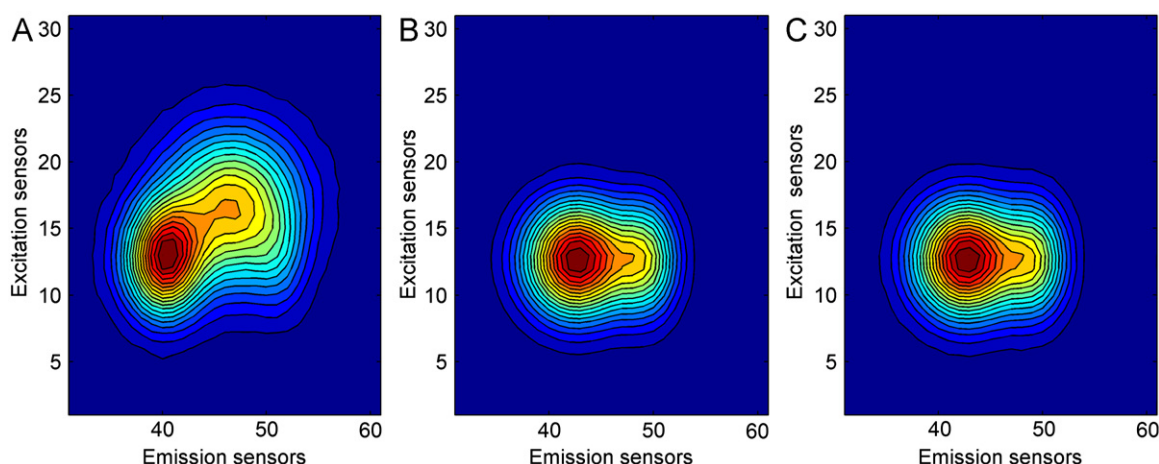
Fig. 3. Contour plots of EEMs from a test sample before (A) and after (B) PDS/PARAFAC procedure and from a calibration sample only containing the component 1 (C).

Table 2
Results and figures of merit of simulated data analysis.

	PDS[c]	SAM[c]
Rec (%)[a]	100 (4) ± 1	99 (3) ± 1
REP (%)[b]	3.7	2.5
SEN [d]	2.2	1.5
γ[e]	221	108
γ^{-1}	0.004	0.009

[a] Mean recovery (%).

[b] Relative error of prediction (%), $REP = \frac{100}{\bar{c}}\left[\frac{1}{I}\sum_{1}^{I}(c_{act}-c_{pred})^2\right]^{1/2}$, where I is the number of samples, c_{act} and c_{pred} are the actual and predicted concentrations, and $\bar{c}$ is the mean concentration.

[c] Between parenthesis the standard deviation.

[d] Mean sensitivity.

[e] Mean analytical sensitivity.

where $\mathbf{B}_{unx}$ and $\mathbf{C}_{unx}$ contain the profiles for the unexpected components as columns, and $\mathbf{I}$ is an identity matrix. Notice that the matrices $\mathbf{B}_{unx}$ and $\mathbf{C}_{unx}$ can be built with columns representing the true spectral profiles for the unexpected components.

Better insight is furnished by the analytical sensitivity, defined by

$$\gamma_n = (SEN_n/||\delta r||) \qquad (13)$$

where $||\delta r||$ is a measure of the instrumental noise, which can be estimated by statistical analysis of blank samples replication. It allows comparing analytical methods, regardless the specific technique equipment and scale employed. Moreover, it establishes the minimum concentration difference (γ^{-1}) which is statistically discernible by the method along the dynamic range, considering the random instrumental noise as the only source of errors.

In the present report, the above defined figures of merit were selected to gather knowledge about the convenience or not of the implementation of the discussed methodology to reduce experimental work and to improve the sensitivity. Thus, the main difference between the methods can be visualized in Table 2 when the analytical sensitivity is considered. As can be seen, this value increased more than two fold when PDS/PARAFAC was applied. Consequently, its inverse, which means the minimum concentration difference that can be measured, was dropped from 0.009 to 0.004 (arbitrary unity of concentration).

An important observation should be made: as the transformation matrix (built with information of the analyte without and with inner filter effect) is used to transfer the sample unfolded data matrix, one want to know if the interference spectrum is modified during this process. Thus, in order to compare the profiles of the interferent obtained after the application of both methodologies with its pure spectra, the degree of spectral overlap (S_{12}) was calculated employing the following expression:

$$S_{12} = \frac{||\mathbf{s}_1{}^T\mathbf{s}_2||}{||\mathbf{s}_1||||\mathbf{s}_2||} \qquad (14)$$

in which $\mathbf{s}_1$ and $\mathbf{s}_2$ are the pure spectra for the interferent and the profile obtained in each case, respectively. The value of S_{12} ranges from zero to one, corresponding to the extreme situations of no overlapping and complete overlapping, respectively. In the excitation mode, the S_{12} values were 0.9256 and 0.9999 for PDS/PARAFAC and SAM, respectively, whereas they were 0.9038 and 1.0000 when the emission mode was analyzed for PDS/PARAFAC and SAM, respectively. The latter indicates that the spectrum of the interferent is slightly modified, although this fact does not exerts a high influence on the analytical figures of merit (see Table 2).

4.2. Experimental data

EEMs were recorded for calibration and validation samples in order to build a second-order model. The three dimensional plots of fluorescence signals, as a function of emission and excitation wavelengths, in absence and in presence of PAR (10.0 ng mL^{-1}), are shown in Fig. 4A and B, respectively. A significant decrease in the emission intensity of PHE can be observed in presence of PAR, due to the inner filter caused by the latter. This behavior can also be observed in Fig. 4C, in which PHE calibration curves at $\lambda_{ex}=215$ nm and $\lambda_{em}=305$ nm, in absence and presence of PAR (10.00 mg L^{-1}) are plotted, being the difference between both slopes evident. In addition, a small shift between the peaks in the emission spectra of PHE with or without PAR can be seen in Fig. 4D. Therefore, the strategy under study has been proposed to solve the inner filter effect and the presence of unexpected compounds whose spectra are severely overlapped with the signal of the target analyte.

The number of responsive components to be included in PARAFAC model was selected by the core consistency analysis [44]. In all cases, the number of components in the validation
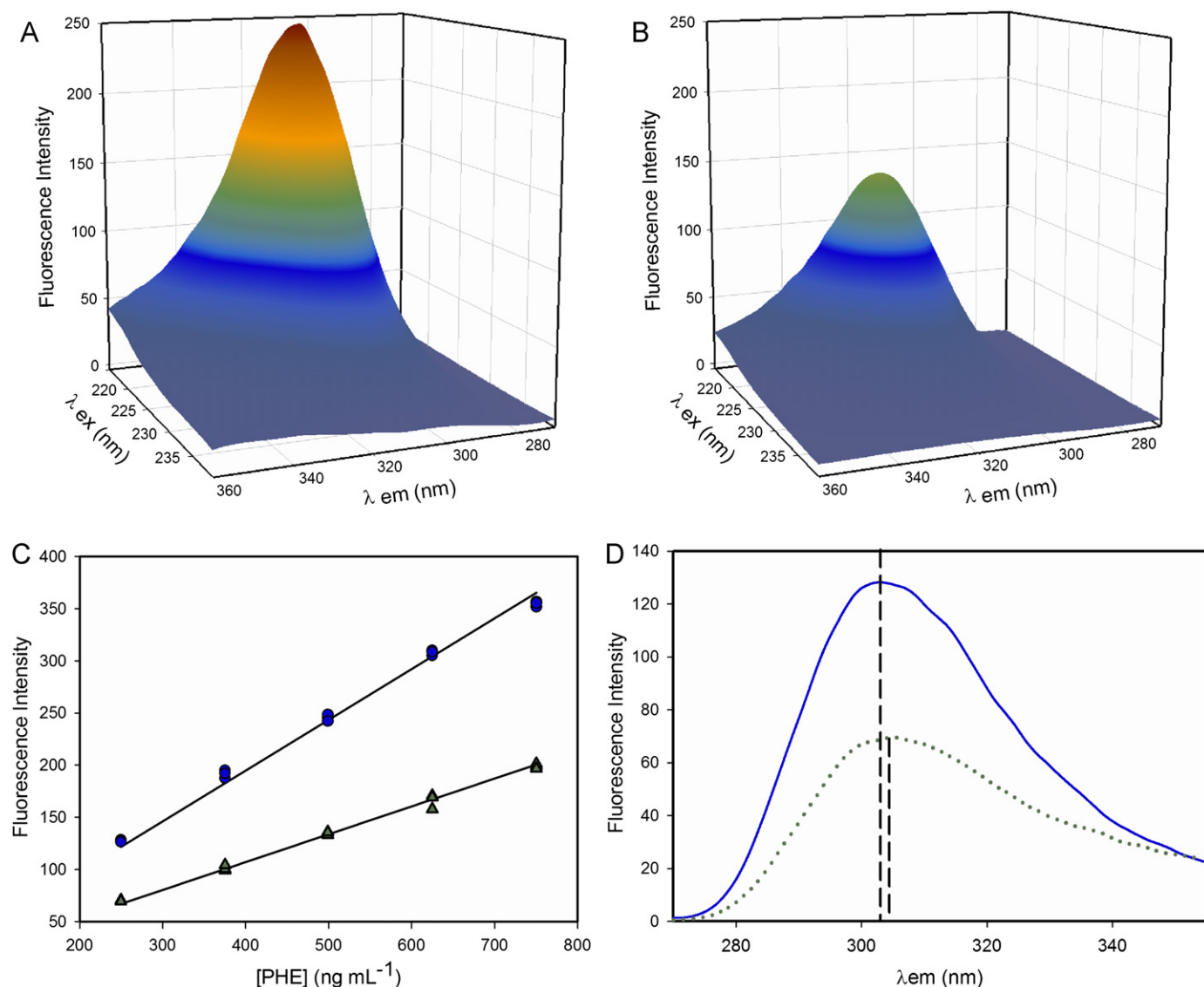
Fig. 4. Three-dimensional plots of fluorescence signals as a function of emission and excitation wavelengths for a calibration sample containing 500 ng mL^{-1} of PHE in absence (A) and in presence (B) of PAR (10.00 mg L^{-1}). (C) PHE calibration curves at λ_{ex}=215 nm and λ_{em}=305 nm in absence (circles) and in presence (triangles up) of PAR (10.00 mg L^{-1}). (D) Standard PHE (250 ng mL^{-1}) emission spectra without (solid line) and with PAR (dotted line).

samples was three, attributed to the fluorescence signals of PHE, IBU and ASA. As PAR is not intrinsically fluorescent in aqueous solutions, it did not interfere, but it caused inner filter effect. The application of PDS/PARAFAC to the experimental data followed the same steps described for simulated data (Section 4.2).

SAM combined with PARAFAC was also applied to samples 2, 12 and 14 from experimental data in order to compare the results. Table 3 shows the prediction results of the validation set with seventeen samples containing different mixtures of PHE, IBU, ASA and PAR (see Table 1). As can be seen, mean recovery values are highly satisfactory for the strategy under study and comparable with those from SAM.

The significance of the comparison of the relative error of prediction (REP) values (REP=4% for SAM/PARAFAC and REP=5% for PDS/PARAFAC) was tested using the randomization approach described in Ref. [48]. Specifically, the use of the randomization *t*-test for the comparison of the REP yields significance level higher than 0.05 (calculated using 1999 iterations, for details see Ref. [48]). This probability indicates that the REP for SAM is statistically equal to the REP for PDS/PARAFAC. Hence, it could be

concluded that the performances of the proposed method is comparable with the standard addition method.

It is important to stand out that different values of slope are obtained for the different levels of PAR (data not shown). Consequently, different standard addition curves must be made for each sample coming to the laboratory, which involves at least four different concentrations of pure standard to be added. As was stated above, the influence of the compound causing the inner filter effect was modeled by Escandar et al. with U-PLS/RBL achieving excellent results, but it should be remarked that this can only be done when interferent causing the inner effect filter is known [20,21].

In the case studied herein, which would call for a complete SAM (i.e., five triplicate standard additions if the IUPAC recommendation are followed [1,3]) only two additions without replicates have to be done to the sample in order to apply PDS/PARAFAC. This strategy reduces the experimental work but still maintains acceptable figures of merit since the same calibration curve (five levels in triplicate) built in Milli-Q water is used for sample prediction. Furthermore, Table 3 shows that the analytical

Table 3
PHE prediction results for the experimental validation set.

Sample	PDS[a] (ng mL⁻¹)	SEN	γ (mL ng⁻¹)	γ^{-1} (ng mL⁻¹)	SAM[a] (ng mL⁻¹)	SEN	γ (mL ng⁻¹)	γ^{-1} (ng mL⁻¹)
1	380(3)							
2	393(4)				361(3)	0.19	0.32	3.1
3	325(4)							
4	259(3)							
5	315(4)							
6	375(6)							
7	285(3)							
8	389(5)							
9	308(2)	0.3	0.4	2.5				
10	341(1)							
11	378(2)							
12	239(9)				238(3)	0.16	0.30	3.3
13	312(2)							
14	343(3)				337(9)	0.22	0.25	4.0
15	342(2)							
16	289(3)							
17	287(3)							
Rec (%)[b]	102 (5)				100 (5)			
REP (%)[c]	5				4			

[a] Between parenthesis the standard deviation of prediction.

[b] Mean recovery (%), between parenthesis the standard deviation.

[c] Relative error of prediction, REP $= \frac{100}{\bar{c}}\left[\frac{1}{I}\sum_{1}^{I}(c_{act}-c_{pred})^2\right]^{1/2}$, where I is the number of samples, c_{act} and c_{pred} are the actual and predicted concentrations, and $\bar{c}$ is the mean concentration.

Table 4
PHE prediction results for water samples.

Component	Sample			
	Tap water		Well water	
	Spiked	Predicted[a]	Spiked	Predicted[a]
PHE (ng mL⁻¹)	306.6	297 (5)	499.8	484 (5)
	306.6	293 (6)	499.8	493 (7)
	306.6	304 (5)	499.8	491 (6)
IBU (ng mL⁻¹)	397.7	–	299.9	–
AAS (ng mL⁻¹)	70.8	–	50.6	–
PAR (mg mL⁻¹)	13.0	–	11.0	–
Mean recovery (%)	–	97	–	98

[a] Between parenthesis the standard deviation of prediction ($n=3$). Three independent samples were predicted during three consecutive days.

sensitivity is once again increased as the inner filter effect is eliminated from the sample signal by applying PDS.

4.3. Water samples

The described methodology was applied to the determination of PHE in two different water samples, i.e., tap water and well water (Table 4). As the EEMs corresponding to the analyzed samples showed that they contained no detectable amounts of PHE, IBU and ASA, spiked samples were prepared at the nominal concentration for IBU and ASA, which are informed in Table 4. It should be noted that sensitivity changes due to the sample matrix were present in these real samples. In addition, PAR was also added to real samples, increasing their complexity. In order to evaluate repeatability and intermediate precision, three independent samples were analyzed in triplicate during three consecutive days. Then, ANOVA tests were applied to each level of concentration to analyze if the differences in the mean values among the three day were not great enough, i.e., if the variation was due to random sampling variability. In could be concluded that there is not statistically

significant difference among the mean values ($p=0.111$ for tap water and $p=0.240$ for well water).

The number of responsive components to be included in PARAFAC model was four in both cases, attributed to the fluorescence signals of PHE, IBU, ASA and an unexpected component from the water samples matrix. Table 4 summarizes the results obtained when different PHE levels were analyzed in real matrices with the presented strategy.

The loadings of the three modes gathered by PARAFAC are observed in Fig. 5, corresponding to the analysis of well water sample. Fig. 5A and B correspond to the excitation and emission mode, respectively, while Fig. 5C shows the relationship between the loadings of the sample mode (scores) and the true concentration of PHE in the calibration samples. The presence of the matrix interference can be attributed to humic substances, such as humic and fulvic acid, which are commonly found in water samples. These molecules are known to be fluorescent since they possess different functional groups [49].

As can be seen, the results are comparable with those obtained for the validation set (Table 3), suggesting that the proposed method is appropriate for the determination of PHE.

5. Conclusion

The methodology herein described shows that it is possible to reduce the experimental work in the determination of an analyte in the presence of unknown compounds and inner filter effect, avoiding the preparation of a large number of solutions and maintaining acceptable figures of merit. This advantage was achieved combining the second-order algorithm PARAFAC with a standardization approach named PDS. Contrarily to previous applications [30–32], a statistical demonstration related to the applicability of the proposed methodology has been performed in the present report. This allowed us to conclude that the presented PDS/PARAFAC constitutes a simple and low-cost strategy for the determination of PHE in water samples with a considerable reduction in standards handling and time. This methodology can be extended to other systems presenting matrix effect and, consequently, can become in a useful tool to know the
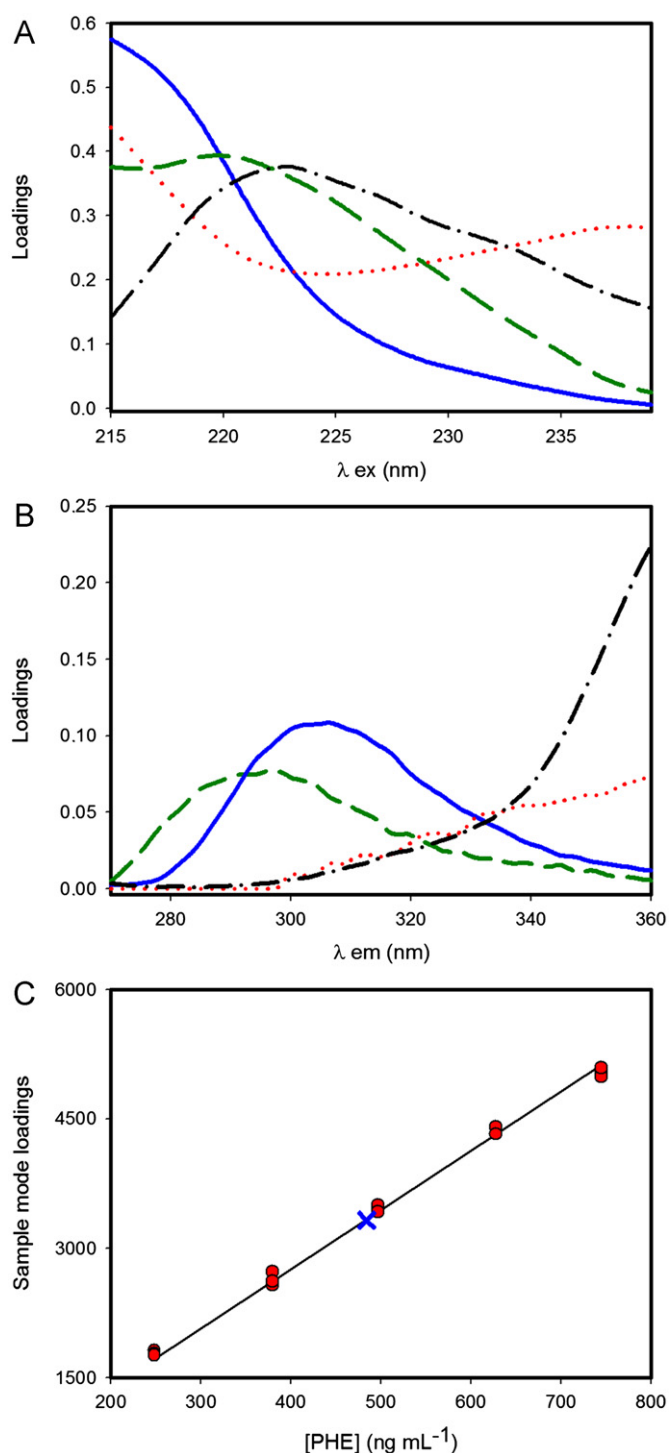
Fig. 5. Modes of the PARAFAC model for PHE (solid line) in the presence of IBU (dashed line), ASA (dotted line) and an unexpected component (dash-dotted line): (A) excitation mode, (B) emission mode and (C) sample mode (circles) in the analysis of transferred well water sample (cross).

amount of pharmaceuticals in the aquatic environment and to evaluate the effect of conventional wastewater treatment plants in the elimination of pharmaceuticals.

Acknowledgments

References

[1] K. Danzer, L.A. Currie, Pure Appl. Chem. 70 (1998) 993–1014.
[2] J.R. Lakowicz, Principles of Fluorescence Spectroscopy, Plenum Press, New York, 1983 44.
[3] R.C. Castells, M.A. Castillo, Anal. Chim. Acta 423 (2000) 179–185.
[4] B.E. Saxberg, B.R. Kowalski, Anal. Chem. 51 (1979) 1031–1038.
[5] A.J. Nepote, A.C. Olivieri, Anal. Chim. Acta 439 (2001) 87–94.
[6] E.C. Silva, V.L. Martins, A.F. Araújo, M.C.U. Araújo, Anal. Sci. 15 (1999) 1235–1240.
[7] F.A. Honorato, R.S. Honorato, M.F. Pimentel, M.C.U. Araujo, Analyst 127 (2002) 1520–1525.
[8] E.C. Silva, M.C.U. Araújo, R.S. Honorato, J.L.F. Costa Lima, E.A.G. Zagatto, S.M.B. Brienza, Anal. Chim. Acta 319 (1996) 153–158.
[9] F. Navarro-Villoslada, L.V. Pérez-Arribas, M.E. León-González, L.M. Polo-Díez, Anal. Chim. Acta 381 (1999) 93–102.
[10] G.M. Escandar, N.M. Faber, H.C. Goicoechea, A. Muñoz de la Peña, A.C. Olivieri, R.J. Poppi, TrAC, Trends Anal. Chem. 26 (2007) 752–765.
[11] F. Cañada-Cañada, A. Espinosa-Mansilla, A. Muñoz de la Peña, A. Jiménez Girón, D. González-Gómez, Food Chem. 113 (2009) 1260–1265.
[12] N. Rodríguez, M.C. Ortiz, L.A. Sarabia, Talanta 77 (2009) 1129–1136.
[13] N. Rodríguez, B.D. Real, M.C. Ortiz, L.A. Sarabia, A. Herrero, Anal. Chim. Acta 632 (2009) 42–51.
[14] P. Valderrama, R.J. Poppi, Chemom. Intell. Lab. Syst. 106 (2011) 160–165.
[15] E. Peré-Trepat, S. Lacorte, R. Tauler, Anal. Chim. Acta 595 (2007) 228–237.
[16] E. Peré-Trepat, S. Lacorte, R. Tauler, J. Chromatogr. A 1096 (2005) 111–122.
[17] V.A. Lozano, R. Tauler, G.A. Ibañez, A.C. Olivieri, Talanta 77 (2009) 1715–1723.
[18] S.-H. Zhu, H.-L. Wu, B.-R. Li, A.-L. Xia, Q.-J. Han, Y. Zhang, Y.-C. Bian, R.-Q. Yu, Anal. Chim. Acta 619 (2008) 165–172.
[19] V.A. Lozano, G.A. Ibañez, A.C. Olivieri, Anal. Chim. Acta 651 (2009) 165–172.
[20] G.N. Piccirilli, G.M. Escandar, Analyst 131 (2006) 1012–1020.
[21] D. Bohoyo Gil, A. Muñoz de la Peña, J.A. Arancibia, G.M. Escandar, A.C. Olivieri, Anal. Chem. 78 (2006) 8051–8058.
[22] R.N. Feudale, N.A. Woody, H. Tan, A.J. Myles, S.D. Brown, J. Ferré, Chemom. Intell. Lab. Syst. 64 (2002) 181–192.
[23] G.G. Siano, H.C. Goicoechea, Chemom. Intell. Lab. Syst. 88 (2007) 204–212.
[24] B. Walczak, E. Bouveresse, D.L. Massart, Chemom. Intell. Lab. Syst. 36 (1997) 41–51.
[25] Y. Wang, D.J. Veltkamp, B.R. Kowalski, Anal. Chem. 63 (1991) 2750–2756.
[26] Y.D. Wang, D.J. Veltkamp, B.R. Kowalski, Anal. Chem. 63 (1991) 2750–2756.
[27] C.V. Di Anibal, I. Ruisánchez, M. Fernández, R. Forteza, V. Cerdà, M.P. Callao, Food Chem. 134 (2012) 2326–2331.
[28] F. Wülfert, W.Th. Kok, O.E. de Noord, A.K. Smilde, Anal. Chem. 72 (2000) 1639–1644.
[29] J. Thygesen, F. van den Berg, Anal. Chim. Acta 705 (2011) 81–87.
[30] M.D. Gil García, M.J. Culzoni, M.M. De Zan, R. Santiago Valverde, M. Martínez Galera, H.C. Goicoechea, J. Chromatogr. A 1179 (2008) 115–124.
[31] M.D. Gil García, F. Cañada-Cañada, M.J. Culzoni, L. Vera-Candioti, G.G. Siano, H.C. Goicoechea, M.Martínez Galera, J. Chromatogr. A 1216 (2009) 5489–5496.
[32] M. Vosough, M. Bayat, A. Salemi, Anal. Chim. Acta 663 (2010) 11–18.
[33] N. Erka, M. Kartal, Farmaco 53 (1998) 617–622.
[34] A. Marín, E. García, A. García, C. Barbas, J. Pharm. Biomed. Anal. 29 (2002) 701–714.
[35] M. Knochen, J. Giglio, Talanta 64 (2004) 1226–1232.
[36] H. Mahgoub, Drug Dev. Ind. Pharm. 16 (1990) 2135–2144.
[37] M.R. Gomez, R.A. Olsina, L.D. Martínez, M.F. Silva, J. Pharm. Biomed. Anal. 30 (2002) 791–799.
[38] J.A. Arancibia, J.A. Nepote, G.M. Escandar, A.C. Olivieri, Anal. Chim. Acta 419 (2000) 159–168.
[39] M.S. Collado, V.E. Mantovani, H.C. Goicoechea, A.C. Olivieri, Talanta 52 (2000) 909–920.
[40] MATLAB 7.1. (2005) The MathWorks Inc., Natick: MA, USA.
[41] B.M. Wise, N.B. Gallagher, R. Bro, J.M. Shaver, W. Windig, R.S. Koch, PLS Toolbox Version 3.5 for use with MATLAB, Eingenvector Research Inc., Manson, USA, 2005.
[42] A.C. Olivieri, H.-L. Wu, E.-Q. Yu, Chemom. Intell. Lab. Syst. 96 (2009) 246–251.
[43] R. Bro, Chemom. Intell. Lab. Syst. 38 (1997) 149–171.
[44] R. Bro, H.A.L. Kiers, J. Chemom. 17 (2003) 274–286.
[45] A.C. Olivieri, N. Klaas, M. Faber, J. Ferré, R. Boqué, J.H. Kalivas, H. Mark, Pure Appl. Chem. 78 (2006) 633–661.
[46] A.C. Olivieri, N. Klaas, M. Faber, J. Chemom. 19 (2005) 583–592.
[47] A.C. Olivieri, N. Klaas, M. Faber, Anal. Chem. 84 (2012) 186–193.
[48] H. van der Voet, Chemom. Intell. Lab. Syst. 25 (1994) 313–323.
[49] N. Senesi, T.M. Miano, M.R. Provenzano, G. Brunetti, Soil Sci. 152 (1991) 259–271.